International Journal of Engineering Innovation & Research
Volume 3, Issue 6, ISSN: 2277 – 5668

Investigating the Impact of Air Temperature on the Performance of a Tesla Turbine - Using CFD Modeling

Ali Hasan, Abdelkader Benzamia

Abstract **– Investigating the impact of fluid gas temperature on a Tesla turbine has recently gained momentum. An example of this isrecovering the energy available in the gas turbine exhaust gas. Tesla turbines, also known as bladeless or boundary turbines were invented in the early 20th century but are rarely used. Bladeless turbines are known for their ease of construction and low erosion rate, since the rotating parts experience no direct impact from the exhaust gas.**

Methodology; A software package was used tocarry out the CFD simulations. The effect of fluid gas temperature and mass flow rate across the turbine were investigated

Results; were tabulated and graphs generated. Equations were derived using an industry established software tool. The accuracy of thedeveloped equations was assessed on statistical basis. Discussions on advantages and disadvantages in using such a turbine were included.

Conclusion; the CFD analysis have shown thatthe fluid gas temperature can affect the efficiency of Tesla turbines. This is due to thefact that the performance of a Tesla turbine is influenced by the boundary layer thickness which is at a maximum when the inter disk spacing equals the boundary layer thickness.Using such a system for energy recovery can lower capital equipment costs and improve the turbine lifespan. Contributing to sustainable engineering development. k-omega turbulence model theory was found tobe suitable model for carrying out this CFD analysis.

Keywords **– Tesla Turbine, Boundary Layer Turbine, Efficiency, Energy Recovery, CFD.**

I. INTRODUCTION

Tesla turbines invented and patented by Nikola Tesla in the early twentieth century have seen little progress in the industry. However this invention is beginning to attract interest in the industry. Main reason being constructions implicity and the turbine suitability in handling various types of fluids. Researchers are now investigating ways to improve the turbine efficiency and establish its limits. Research continues in establishing equations to describe the fluid mechanics of such turbines. This paper uses CFD software to investigate how gas mass flow rate and gas temperature can impact the efficiency of such turbines. Detailed close-up graphical images were produced aimed at giving a better understanding of how Tesla turbines work and how efficiency can be improved by considering fluid gas temperature.

II. TESLA TURBINE

Tesla turbines are typically made of a number of equally spaced disks mounted on a shaft. A number of holes through the disks and around the shaft exist. As the gas enters the turbine casing and flow along the disk surfaces, the disks begin to rotate. Fluid gas entering the turbine casing through the inlet ports in such a way that the gas stream lines contact the outer disk surfaces tangentially and move along the disk surface planes. The fluid viscous drag forces acting on the disks surfaces causing the disks to rotate. This converts hydraulic fluid energy to rotating mechanical energy. As the moving fluids streams pass energy to the rotating disks, fluid pressure begin to drop and then exit through the lower pressure turbine outlets at the centre of the turbine near the shaft. Figure1shows a3D image of the considered Tesla turbine model. Figure 2 shows model dimensions for a single inlet port. Figure 3 shows how such turbines can be arranged with a different number of equally spaced out fluid gas inlet ports. Models shown in Fig 1 and 3 have the same dimensions of what is shown in Fig 2, but with one inlet port basically rotated in the software modeler to obtain the different equally spaced number of inlet ports.

A paper by Piotr Lampart and Łukasz Jędrzejewski [1] states that the inventor of the blade less turbine or pumps patented his invention in 1913. The invention did not progress into major production work, but is currently attracting interest by researchers and manufacturers in the industry.

The turbine is generally simple to construct, and the amount of machining works are relatively low when compared with other turbines. Centrifugal turbines as an example have more complex geometry. Hobbyists interested in Tesla turbines are known to have constructed such a turbine using computer Compact Disks. A paper by Nam Spencer states [6], despite its inefficiencies, the Tesla turbine still has several advantages. The production costs for disks are much lower than for blades, and the overall design is simpler and more easily manufactured.

III. CFD MODEL

The model prepared for investigation shown in Fig1 was prepared using Fluent software. Settings not specified in this paper can be left at software default settings. The following settings and assumptions were made:-

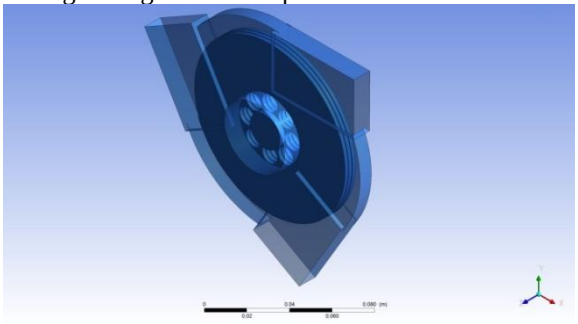

Fig.1. Tesla turbine 3D image with three inlet ports model.

- Fluid; Air was selected from the software data base which is assumed to have similar properties to an engine exhaust gas. Air was assumed as an ideal gas.
  According to ER at hakrishnan [2], many of the familiar gases such as air, nitrogen, oxygen, hydrogen, helium, argon, neon, krypton, and even heavier gases such as carbon dioxide can be treated as ideal gas with negligible error, often less than1%.
- Exhaust gas temperatures; of 100 °C(232 °F), 200 °C(432 °F), 300 °C(632 °F), and 400°C(832 °F), were considered.
  As an example Siemens gas turbine SGT-100 models are known to have an exhaust gas temperature in the region of 545 °C (1013 °F) to 531 °C (988°F). As exhaust gas travels out of the engine outlet and travel through the exhaust gas duct, temperature drops, and therefore lower exhaust temperature were considered for practical reasons.
- Disks, and shaft material; Aluminum selected from the software database. Note: material temperature properties are assumed acceptable for the purpose of simulation, and is not the subject of discussion in this paper.
- Fluent menu; select the Energy option "on", k-omega (a common turbulence model), and the aluminum materials wall roughness constant, 0.5. Appendix 1 shows a description of this model and specific software settings. Solver convergence was set for1000 iterations.
- Shaft speed and torque results; were determined using the CFD postprocessor.
- A suitable meshing was used to build a sufficient layer of cells to fill the inter-disk spacing, and provide a good approximation of surface boundary layer conditions. In this example10,151,627 cells were used to mesh the model shown inFig1.
- Initially one model was simulated with 0.01 kg/s (0.022 lb/s) of gas flow rate per an inlet port at 100 °C (232 °F) and then 0.02 kg/s (0.044 lb/s) per a port, and so on and as shown in Table 1.
- Inter-disk spacing was initially set at 0.4 mm (0.016 inch). According to Wikipedia [3], steam powered type must maintain 0.4 mm (0.016 inch) inter disk spacing. Though the fluid in this case is exhaust gas and not steam.
- Outlet pressure was assumed at standard absolute atmospheric pressure,1 bar.

IV. Results and Calculations

This section is divided into two parts. First assessing the CFD generated results and comparing them with theoretical boundary layer thickness conditions, and then, assessing the boundary layer condition using established equations.

Assessing the CFD results

Results produced at the post processing stage were tabulated as shown in Table 2. Graphical model images showing; velocity contours, velocity streamlines, and temperature volume rendering are shown in Figs 4 to 6 respectively. Figures 7 and 8 show close-up images of fluid streamlines moving across the turbine disk surfaces and then exiting through the central outlet ports.

Graph plot Figs 9 and 10, show the relationship between shaft power and efficiency with respect to gas flow temperature. The graphs are based on the two highest efficiency figures achieved in Table 1. These graphs show the effects of exhaust gas temperature on turbine shaft power and efficiency.

Equations were developed by employing curve

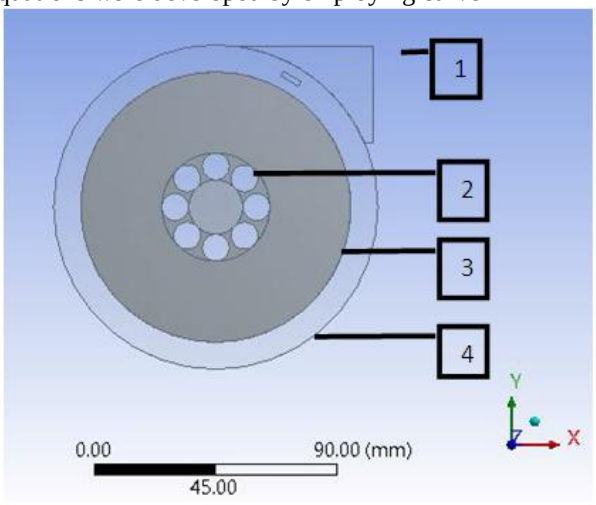

(a)

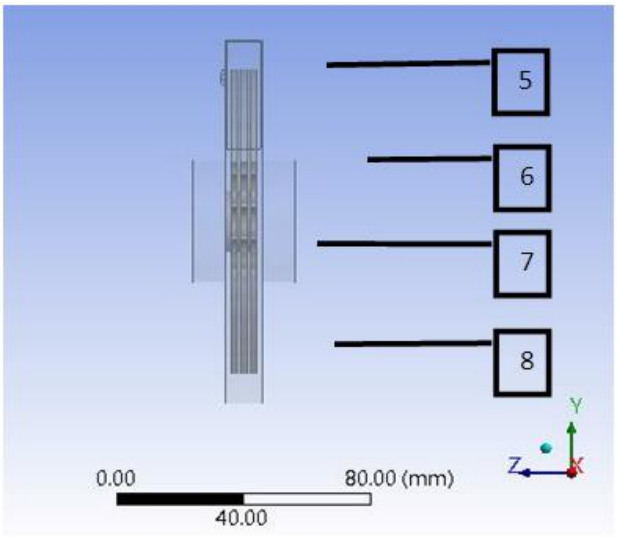

(b)

Fig.2. Example of a single port inlet model. (a) Side view of turbine with dimensions as shown. (b) Front view of turbine with dimensions.

Note: A single port inlet was selected for clarity of description.

Dimensions:

1- Inlet face projected 120 mm (4.8 inch) from disk y-axis.
2- Disk circular holes 10 mm (0.4 inch) diameter. Centre of holes 15 mm (0.6 inch) from disk central axis.
3- Disk diameter 100 mm (0.4 inch), 2 mm (0.08 inch) thick.

4- Outer casing diameter 120 mm (4.8 inch).
5- Inlet port face dimensions 10 mm (0.4 inch) by 35 mm (1.4 inch).
6- Outlets on both sides, diameter 40 mm (1.6 inch). Face extended 10 mm (0.4 inch) from wall casing.
7- Shaft diameter 20 mm (0.8 inch).
8- Casing width varies with case wall to disk surface spacing equal to inter disk spacing.

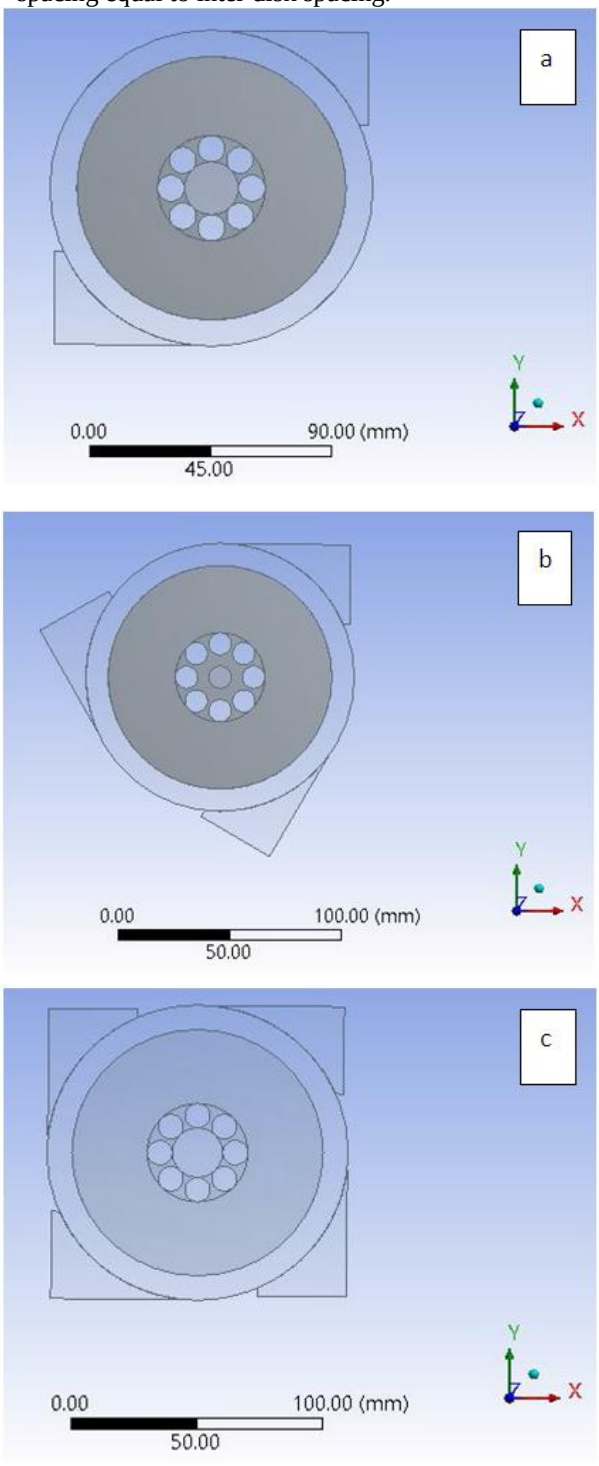

Fig.3. Model with various inlet ports, side views shown. Disks were set to rotate freely about z-axis. As the inlet flow rate and temperature changes turbine performance was observed. (a) Two inlet ports equally spaced out. (b) Three inlet ports equally spaced out. (c) Four inlet ports equally spaced out.

A Three inlet ports model was considered.

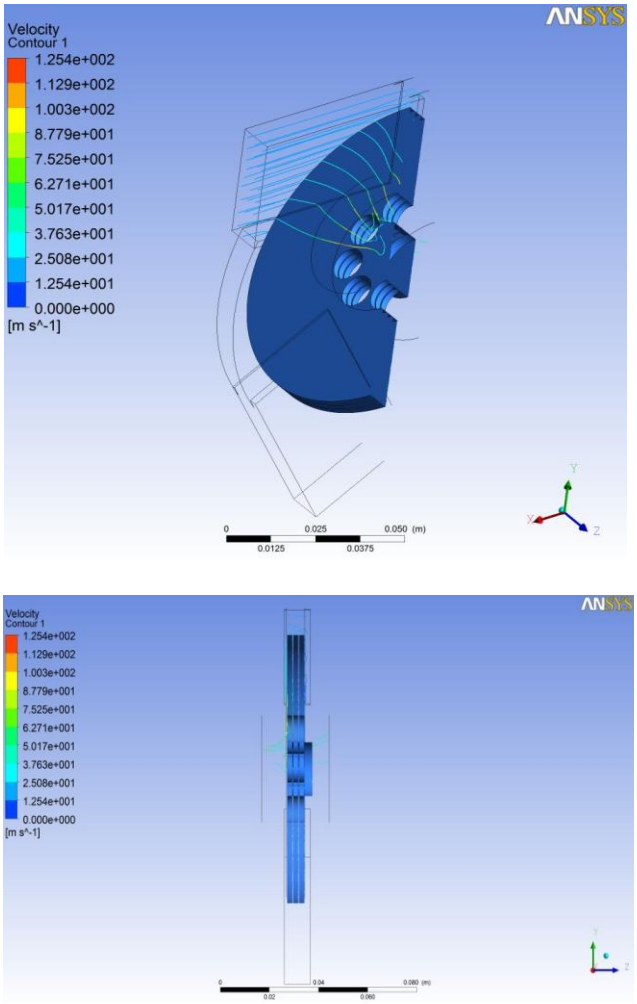

Fig.4. Postprocessor graphics output for a 100 °C (232 °F) gas inlet temperature with a flow rate of 0.01 kg/s (0.022 lb/s) per an inlet port. The streamlines show the path of fluid as it enters the pump inlet and move through the disk openings, and then away from the center of the disks. (Top) Three dimensional sectional views shown with velocity streamline. (Below) Front sectional view of the above picture, with velocity streamlines.

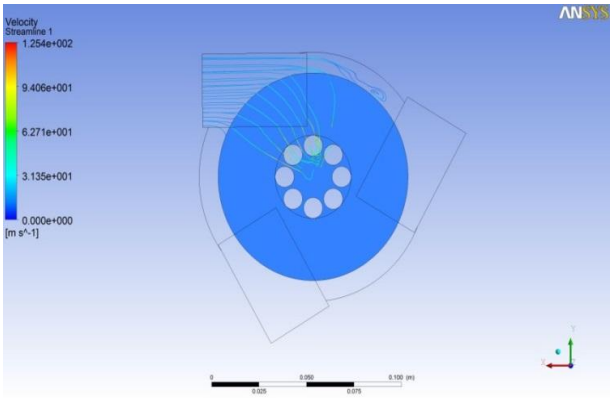

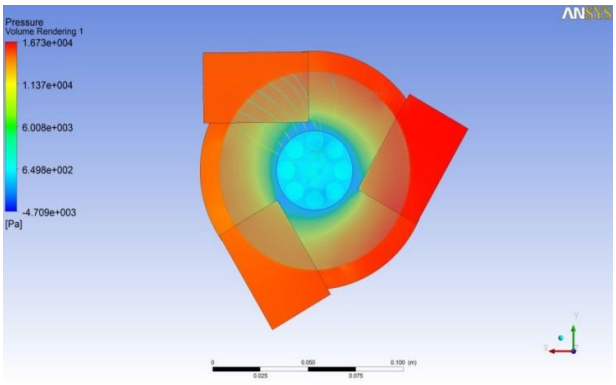

Fig.5. Postprocessor graphics output for a 100 °C (232 °F) gas inlet temperature with a flow rate of 0.01 kg/s (0.022 lb/s) per an inlet port. Disk rotating clockwise under the action of fluid gas flow. (Top) Velocity streamlines tracked from one inlet port. (Below) Pressure volume rendering image shows relatively high pressure near the inlets, and then the gas pressure gradually drops towards the outlet. This pressure drop represents the transfer of hydraulic fluid energy to mechanical rotational energy.

Fitting - approximation, as shown in Figs 9 to10. The accuracy of the approximated curve fittings hence equations, were assessed on the basis of statistical regression analysis, as described below;

Assessing integrity of formulas developed by regression. With a low R^2= 0 n ne of the variances on the Y axis can be explained against T ºC shown on the X axis. With high R^2=1, all of the variances on the Y axis can be explained against T °C on the X axis. Where R^2, is known as the coefficient of determination.

Shaft power – temperature equation:

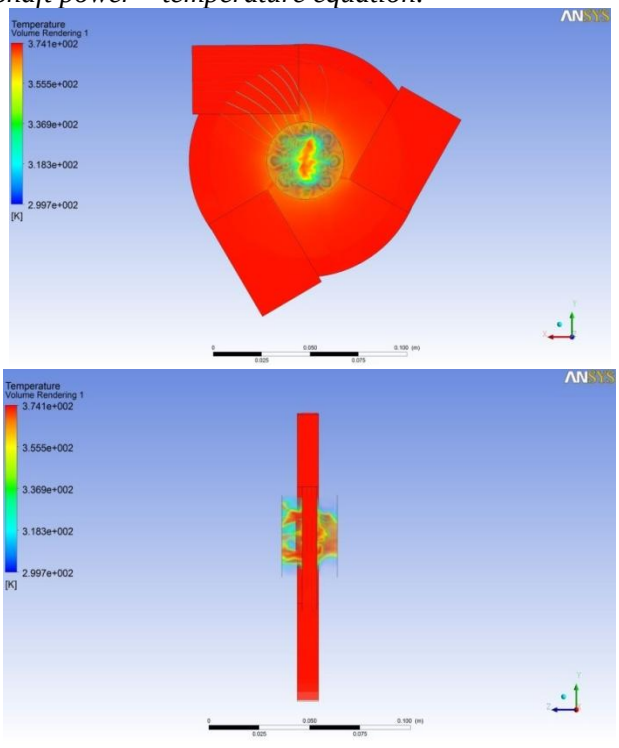

Fig.6. Postprocessor graphics output for a 100 °C (232 °F) gas inlet temperature with a flow rate of 0.01 kg/s (0.022 lb/s) per an inlet port. (Top) Shows temperature rendering model with streamlines selected for one outlet for clarity. Disk rotating clockwise under the action of the inflow gas. (Below) Shows a sectional view of the above picture along the y-axis. The relatively lower gas temperature near the outlet is clearly visible. At this point the hot gas has lost some of its energy, to the rotating disks.

For 0.01 kg/s (0.022 lb/s)

P_S=3E-07T^3- 0.0003 T_G^2+0.0626 T_G- 3.944 (1a)

R^2=1

See Fig 9 for relevant curves

For 0.02 kg/s (0.044 lb/s)

P_S=-7E-08T_G^3+6E-05T_G^2- 0.0103 T_G+1.4132 (1b) (1b)

R^2=1

R^2=1

See Fig 9 for relevant curves

Efficiency – temperature equation:

For 0.01 kg/s (0.022 lb/s)

Efficiency=-9E-06T_G^3+0.0085 T_G^2- 2.5674 T_G+253.99 (2a) (2a) R^2=1

R^2=1

See Fig 10 for relevant curves

For 0.02 kg/s(0.044 lb/s)

Efficiency = 9E-06T_G^2- 0.005 T_G+2.4583 (2b)

R^2=0.6983 (2b) R^2=0.6983

See Fig 10 for relevant curves

Assessing boundary layer thickness – theoretical:

Graph Fig11 was used to generate equations (3a) and (3b), which can be used to determine δ. Graph 11 was plotted from Table 3. Equations (4) to (8) were used to produce Table 3. The Re value can be used to determine whether the laminar or turbulent curve should be used.

Laminar flow equation:

δ=-2E-07T_G^2+0.0007 T_G+0.232 (3a)

R^2=1 (3a) R^2=1

SeeFig11 for relevant curves.

Turbulent flow equation:

δ=-3E-07T_G^2+0.0006 T_G+0.5726 (3b)

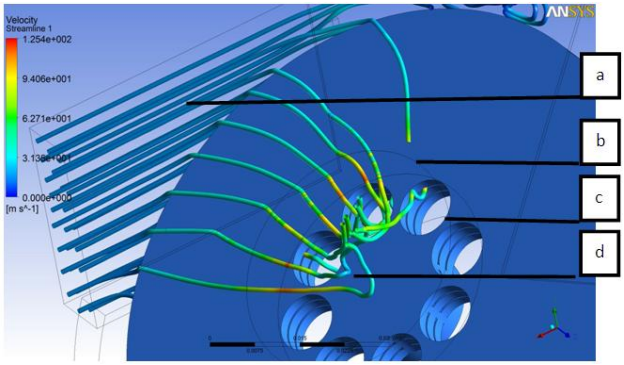

Fig.7. A close-up view of a 0.01 kg/s hot gas 100 C (232 F) supplied through the turbine port. This image shows

how a Tesla-type turbine works, boundary conditions and the fluid's viscosity physics are utilized. The turbine casing texture switched-off and disk's image presented for clarity. The velocity streamlines indicate the path of gas movement.

a-This image shows an example of how hot gas enters the turbine pump casing. b-The fluid then moves through the disk spacing and along the disks surface. c- Fluid moves out of the holes around the turbine shaft.Note: At point gas velocity is at 95 m/s (311.6 ft/s). d- Finally out through the outlet.

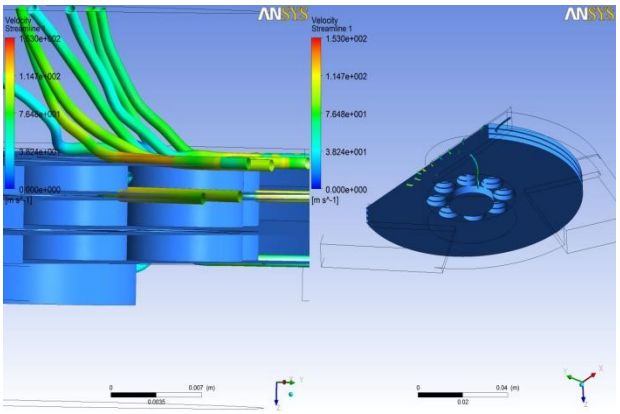

Fig.8. Shows images with velocity streamlines, 200 °C

(432 °F) gas temperature, 0.01 kg/s (0.022 lb/s) gas flow rate per an inlet. (Right) Shows a 3D image at an angle with a portion of the disks sliced to allow for the viewing of "in-between" disks velocity streamlines. (Left) shows a zoomed-in image of the cut through image shown on the right hand side. This allows for a close up image, showing the velocity streamlines. Streamlines indicate a range of velocities in between 50 and 150 m/s (164 and 492 ft/s). See end sections in discussions.

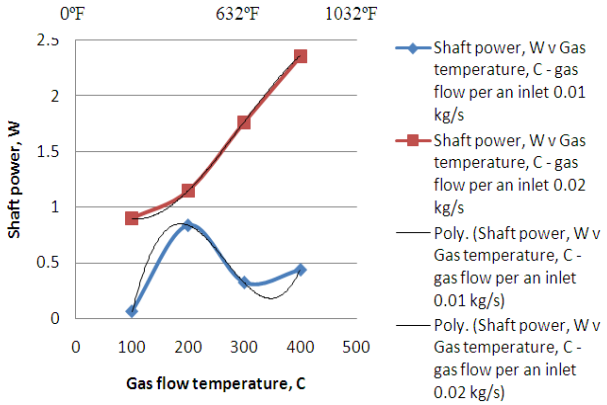

Fig.9. Shaft power v gas flow temperature for 0.01 kg/s (0.022 lb/s) and 0.02 kg/s (0.044 lb/s) per an inlet. Curve fitting approximations are "Poly" curves. Data plotted from Table 2.

Table 1: Calculating Boundary layer thickness, δ, for the purpose of optimizing inter-disk spacing.

Temperature, °C	Dynamic Viscosity, kg/m.s	Density, kg/m^3	Velocity, m/s	X, m	Re	δ if Laminar, mm	δ if Turbulent, mm
100	2.18E-05	0.946	94	0.015	61186.2	0.3032	0.63216
200	2.58E-05	0.7461	94	0.015	40775.2	0.37142	0.68561
300	2.93E-05	0.6159	94	0.015	29638.9	0.43564	0.73077
400	3.25E-05	0.5243	94	0.015	22746.6	0.49728	0.7705

Temperature, °F	Dynamic Viscosity, $lb_f.s/ft^2$ e7	Density, lb/ft^3	Velocity, ft/s	X, inch	δ if Laminar, inch	δ if Turbulent, inch
232	4.49	6	308.32	0.0006	0.01213	0.02529
432	5.24	4.6	308.32	0.0006	0.01486	0.02742
632	6.3	3.38	308.32	0.0006	0.01743	0.02923
832	7	3.2	308.32	0.0006	0.01989	0.03082

Top table forms the basis of calculations for determining δ. Boundary layer thickness or δ was calculated as discussed in the Results and Calculations section.

Lower table shows figures in imperial units. Values for dynamic viscosity and density were obtained from a book by Professor E Rathakrishnan.

Table 2: CFD results and calculations.

T_G, °C (°F)	ṁ, kg/s (lb/s)	ρ, kg/m^3 (lb/ft^3)	Q_T, m^3/s (ft^3/s)	*h, m (ft)*	S, rad/s	T, Nm (lb.ft)	P, W	Efficiency %
100 (232)	0.01 (0.022)	*0.946* *(0.59)*	*3.17E-02* *(1.12)*	2.596 (8.51)	500	4.56E-04 (0.00034)	0.0601789	73
200 (432)	0.01 (0.022)	*0.7461* *(0.046)*	*4.02E-02* *(1.42)*	2.8384 (9.31)	620	5.18E-03 (0.0038)	0.8390515	7
300 (632)	0.01 (0.022)	0.6159 (0.038)	4.87E-02 (1.72)	3.4402 (11.28)	752	1.62E-03 (0.0012)	0.3215302	2

400 (832)	0.01 (0.022)	0.5243 (0.033)	5.72E-02 (2.02)	3.869 (12.69)	880	1.88E-03 (0.0014)	0.4364918	2
100 (232)	0.02 (0.044)	0.946	6.34E-02 (2.24)	6.8071 (22.33)	912	3.74E-03 (0.0027)	0.8979264	2
200 (432)	0.02 (0.044)	0.7461	8.04E-02 (2.84)	8.3079 (27.25)	1140	3.82E-03 (0.0028)	1.146591	2
300 (632)	0.02 (0.044)	0.6159	9.74E-02 (3.44)	9.7845 (32.09)	1326	5.19E-03 (0.0038)	1.764498	2
400 (832)	0.02 (0.044)	0.5243	1.14E-01 (4.03)	11.1948 (36.72)	1528	5.89E-03 (0.0043)	2.356976	2

Table 3: Table showing calculated values for δ using equations (4) to (8).

v, m/s	Re	δ Laminar, mm	δ Turbulent, mm
50	3.25E+04	4.16E-01	7.17E-01
60	3.91E+04	3.80E-01	6.92E-01
70	4.56E+04	3.51E-01	6.71E-01
80	5.21E+04	3.29E-01	6.53E-01

See Fig 8 for velocity streamline figures through the inter-disk spacing. Above table calculates the theoretical boundary layer thickness using equations 4 to 8. Selected set inter-disk spacing in this case 0.4 mm (0.016 inch) can be adjusted to match the above calculated boundary layer thickness for optimizing purposes. Where x, distance from the start of boundary layer is 15 mm (0.6 inch).

$R^2=1$

See Fig11 for relevantcurves.

Accordingly to Wikipedia the boundary layer thickness for laminar flow can be calculated by the equation developed by Paul Richard Heinrich Blasius;

$$\delta = (5.0 \times x) \div \sqrt{Re} \qquad (4)$$

Where $Re=(\rho \times v_\infty \times x) \div \mu$ (5)

Rearrange (4) to obtain Re, hence provide an estimate on flow rate, by determining

The velocity component, v_∞, given in equation (5);

$$\sqrt{Re} = (5.0 \times x) \div \delta \qquad (6)$$

Similarly for turbulent flow,

$$\delta = (0.382 \times x) \div {}^{1/5}Re \qquad (7)$$

Re-arrange (7) to obtain Re

$$(Re)^{1/5} = (0.382 \times x) \div \delta \qquad (8)$$

It is clear from equation (4), that δ depends on the Re value, and that as the parameters on the right hand side in equation (5) change the Re values changes. Subsequently influencing the value of δ. The parameters on the right hand side of equation (5) depend on gas temperature. This can be seen in Table 2. Table 2 shows that as temperature of gas increases, the density drops while the dynamic viscosity increases. This table shows the impact of gas temperature on the boundary layer thickness. The following calculations below give an example of how δ the boundary layer thickness is calculated on the basis of 100 °C (232 °F) gas temperature.

Using equations (4) and (7). A value of a streamline gas velocity, in between the disks shown in Fig 7 was selected as shown in Fig 6, which gave 95 m/s (311.6ft/s). Equation (5) was used to assess whether the flow is laminar or turbulent at an approximate distance of 15e-3m (6 inch), as an example:-

$Re = (0.946 \times 95 \times 15e\text{-}3) \div 2.18\ e\text{-}5 = 61186.2$

This Re number indicates turbulent flow, therefore, the turbulent flow equation (7) will be used to determine δ. This establishes the following facts;

- Inter disk spacing in the CFD model was to be 0.4mm (0.016inch) which gave a maximum efficiency of 73 % at100 ºC (232 ºF) with 0.01 kg/s(0.022 lb/s) per an inlet, as shown in Table 2.
- In theory using graph Fig 11, the boundary layer thickness calculated at an approximate distanceof15e-3m (6inches), locations shown in Fig 7, gives 0.63216 mm (0.0253 inch).

Since it is known that efficiency of such turbines depends on getting the boundary layer thickness to equal inter disk spacing, it can be said that there is room to improve efficiency further, by changing the inter disk spacing to be 0.63mm (0.025inch). Bearing in mind that accuracy of the CFD results is influenced by mesh density and the turbulence model used.

See section on discussions in relation to the subject on boundary layer thickness and inter- disk spacing.

V. DISCUSSIONS

According to Earl Loganand Warren Rice of Arizona State University [4], Tesla designed, built, and tested such machines but was not able to achieve industrial applications of them. In the subsequent years, many investigations have been carried out to determine the performance and efficiency of such turbo machinery. These investigations have been both analytical and experimental. Most of the investigations have had a certain limited application as the objective, with regard to size and speed as well as the nature of the operating fluid. However, some of the investigations have tried to establish the generalized performance of Tesla-type turbo machines. In general it has been found that the efficiency of the rotor can be very high, at least equal to that achieved by conventional rotors. But it has proved very difficult to achieve efficient nozzles in the case of turbines. For pumps and compressors, efficient diffusions after the rotor has proven difficult to achieve. As a result, only modest machine efficiencies have been demonstrated. Principally for these reasons the Tesla-type turbo machinery has had little utilization. There is, however, a wide spread belief that it will find applications in the future, at least in

situations in which conventional turbo machinery is not adequate. This includes the use with very viscous fluids, fluids containing abrasive particles, and two phase fluids.

A description by Malcolm Crockerand Mirko Cudina of the University of Ljubljana Slovenia [5]. Such units are known for working as pumps and turbines with minor adjustments, see text below by Spencer Nam. This indicates the versatility of these machines.

A paper by Piotr Lampart and Łukasz Jędrzejewski, the following factors influence the performance of the turbine or in this case pump;

• Distance between micro-turbine disks.
• Number, diameter and state of the disk surface of micro-turbine disks.
• Number and construction of inlet nozzles.
• Rotational speed of the rotor.
• Medium inlet pressure, temperature, velocity and angle.
• Corrosion and erosion of micro-turbine elements, or pump disks.
• Construction of materials (composites, ceramic materials, bronzes, aluminum alloys).
• Kind of medium flowing through the micro-turbine (air, biogas, organic agents, exhaust gases, multi-phase media).

A paper by Spencer Nam states [6]; the flow of fluid in the turbine can also be reversed into a pump, and the disks do not suffer from capitation issues that bladed turbines often have. These features lend themselves well to potential uses in the generation of power from geothermal steam and particle-laden industrial gas. Other potential uses include blood pumps as well as in wind turbines. Though the Tesla turbine has not yet proven to be more effective than traditional turbines, there are still potential practical uses.

A paper by Metaj Podergajs [7] mentions some of the drawbacks and advantages; other drawbacks are shear losses and flow restrictions. But that can be advantages when flow rates are low. Tesla's design can also be used, when a small turbine is needed. Efficiency maximized when boundary layer thickness is approximately equal to inter disk spacing. So at high flow rates, more disks are needed, which means a larger turbine. Because thickness of boundary layer depends on viscosity and pressure, various fluids cannot be used. Disks need to be as thin as possible to prevent turbulence at disk edges.

Maximum efficiency develops when the inter-disk spacing approximate the thickness of the boundary layer, as stated in Wikipedia.

On the basis of above discussions, the inter-disk spacing used in this model needs to be increased to match the calculated boundary layer thickness. If the gas temperatureis100 °C (232°F), then the 0.4 mm (0.016 inch) inter-disk spacing would need to be increased to Approximately 0.6 mm (0.024 inch). It can be deduced that when considering recapturing energy available in the exhaust gas system, the inter disk spacing of Tesla turbines must consider the exhaust gas temperature as well as the other parameters given by Piotr Lampart and Łukasz Jędrzejewski.

The CFD analysis confirms the advantages of using k-omega turbulence model discussed in Appendix1. Particularly as in this case where fluid boundary layers are the focus of this analysis. Where adverse pressure gradients exist between the near disk wall sub-viscous layer, and fluid boundary layers moving away from the disk walls. The k-omega turbulence model is well known for being; numerically stable, converges more rapidly at low Re values. Low Re values near disk walls exist due to the relatively lower fluid velocity movement near disk walls. A description on the importance of boundary layers moving along solid surfaces is covered in the following paragraph.

B.S. Massey [8] describes flow near the boundary layer may be either laminar or turbulent. Turbulent flow past a solid surface having a random movement of particles perpendicular to the surface. Yet fluid particles cannot pass through an impermeable solid surface, and so, as the surface is approached, these movements perpendicular to it must die out. It follows then that turbulent flow cannot exist immediately in contact with the solid boundary.

Thus even when main flow possess considerable turbulence, and even when the greater part of the boundary layer is also turbulent, there is still an extremely thin layer, adjacent to the solid surface, in which the flow has negligible fluctuations of velocity. This region, which may be less than a micron in thickness, has frequently been called the laminar sub-layer, but the term viscous sub-layer is now preferred. It is this low-Reynolds- number extension for near-wall turbulence covered in Appendix 1 which improves solver convergence and CFD analysis.

VI. CONCLUSION

The CFD simulation was carried out successfully with the following facts determined.

- For maximized efficiency, Tesla turbines inter-disk spacing must be equal to the boundary layer thickness produced by the gas flow, which inherently depends on the fluid gas temperature and not just the type of fluid.
- Tesla turbines efficiency depends on the following factors:

a. Fluid type, dynamic viscosity and density.
b. Fluid temperature.
c. Number of disks.
d. Disks surface finish.
e. Disk thickness.
f. Disks surface areas.
g. Disks exhaust openings.

- CFD analysis can be used to optimize inter-disk spacing for a specific fluid flow and temperature. Optimizing performance by setting the inter-disk spacing to match the fluid boundary layer thickness.
- Specifying k-omega Turbulence Model, and Intensity & viscosity ratios at the inlet and outlets produced stabilized results during the processing stage.

ACKNOWLEDGMENT

- Mr Abdelkader Benzamia of Flowpak, Flowpak, Doha, Qatar, www.flowpak.net,for the guidance and input on best practices in CFD meshing.
- Siemens Energy– gas power turbines. For information on gas turbine exhaust temperature.

REFERENCES

[1] Paperby Piotr Lampart and Łukasz Jędrzejewski. Papertitle, Investigations of Aerodynamics of Tesla Blade less Micro-turbines. 25 November 2010. Polish Academy of Science Gdansk.
[2] Author E Rathakrishnan, Title; Gas Dynamics. Fifth edition. Publisher PHI.
[3] Wikipedia, Nikola Tesla.
[4] Earl Logan and Warren Rice of Arizona State University, With Permission from Elsevier.
[5] Malcolm Crocker and Mirko Cudina of the University of Ljubljana Slovenia, page 897, Hand Book of Noise and Vibration Control. Published by John Wiley and Sons Inc, USA.
[6] Paperby Spencer Nam. Papertitle, The Tesla Turbine. 14 December2012. With permission from IHS.
[7] Paperby Metaj Podergajs. TheTeslaTurbine.March2011. University of Ljubjana, Slovenia.
[8] B.S. Massey, Title; Mechanics of Fluids. Fifth edition. Publisher Van Nostrand Reinhold (UK).
[9] Professor Brian Spalding, POLIS Encyclopedia, CHAM. Wimbledon. London, UK. (2014).
[10] Wikipedia – section on k-omega turbulence model.

APPENDIX I

Specific CFD software setup is shown in this section. Other setups not described here shall be as per software default settings.

Turbulence Model used

A brief description of k-omega or k-ω turbulence model is given by Professor Brian Spalding [9] is shown below;

Although the k-ω model is not as popular as the k-epsilon or k-ϵ model, it does have several advantages, namely that:

a) the model is reported to perform better in transitional flows and in flows with adverse pressure gradients. *This explains the successful usage of this model in this paper, where adverse pressure gradients exist. Particularly between the low velocity or Re value of fluid boundary layers close to the disk surfaces, and fluid boundary layers away from the disk surfaces.*

b) the model is numerically very stable, especially the low-Re version, as it tends to produce converged solutions more rapidly than the k-epsilon turbulence models; and

c) the low-Re version is more economical and elegant than the low-Re k-epsilon models, in that it does not require the calculation of wall distances, additional source terms and/or damping functions based on the friction velocity.

The main weakness of the k-ω model is that unlike the k-ϵ model, it is sensitive to the free-stream boundary condition for ω in free-shear flows. Modified variants exist which claim to remove this sensitivity, such as the Shear Transport turbulence model theory (SST). Since in this example the inter disk spacing is small another words does not involve free streams, this sensitivity to free-shear flows was neglected in this analysis.Equations and description shown below, also given in Wikipedia [10] k-omega turbulence model (2014) section;

$$\frac{\partial(\rho k)}{\partial t}+\frac{\partial(\rho u_j k)}{\partial x_j}=P-\beta^*\rho\omega k+\frac{\partial}{\partial x_j}\left[\left(\mu+\sigma_k\frac{\rho k}{\omega}\right)\frac{\partial k}{\partial x_j}\right]$$

$$\frac{\partial(\rho\omega)}{\partial t}+\frac{\partial(\rho u_j\omega)}{\partial x_j}=\frac{\gamma\omega}{k}P-\beta\rho\omega^2+\frac{\partial}{\partial x_j}\left[\left(\mu+\sigma_\omega\frac{\rho k}{\omega}\right)\frac{\partial\omega}{\partial x_j}\right]+\frac{\rho\sigma_d}{\omega}\frac{\partial k}{\partial x_j}\frac{\partial\omega}{\partial x_j}$$

K-omega (k-ω) turbulence model is a common two-equation turbulence model in computational fluid dynamics that is used as a closure equation of the Reynolds-averaged Navier–Stokes equations. The model attempts to predict turbulence by two partial differential equations with the first variable being the turbulence kinetic energy while the second being the specific rate of dissipation.

The first transported variable is turbulent kinetic energy, k. The second transported variable in this case is the specific dissipation, ω. It is the variable that determines the scale of the turbulence, whereas the first variable, k, determines the energy in the turbulence.

Specific model settings were based on k-ω for turbulence models and inlet and outlet conditions.

Inlet and outlet turbulence specifications used

At the inlet boundary mass flow inlet, Intensity and viscosity ration was selected. Turbulence intensity set to 1%, and 10 for viscosity ratio.

At the outlets, the pressure outlet menu was opened. Intensity and viscosity ration was selected, Turbulence intensity set to 10%, and 10 for viscosity ratio.

Elements Quality

The quality of the mesh plays a significant role in the accuracy and stability of the numerical computation. The orthogonal quality is checked and the following results were recorded. Minimum = 8.43e-2; Maximum = 1.00; Average = 0.83; Standard Deviation = 0.105

A cell having an orthogonal quality close to zero indicated bad quality, while a cell having an orthogonal quality close to indicate high quality. The average orthogonal value is 0.85 which is good.

NOTATION

CFD =Computational Fluid Dynamics. ANSYS Fluent=CFD software brand. mm=millimeters. m=meters. ft/s = feet per a second. kg/s=kilograms per a second. C,&F =Degrees centigrade, and degrees Fahrenheit. M^3/s=cubic meters per a second. Nm= Newton meters. ft=feet.cfs =cubic feet per a second. lb. ft=pounds. feet. rad/s=radians per a second. rpm=revolutions per a minute. P =pressure. Q =Inlet flow. Re=Reynolds number. δ =Boundary layer thickness. μ =Dynamic viscosity. ρ =density of fluid. v =velocity of fluid. x =distance from start of boundary layer. ṁ = mass flow rate. T_G=Temperature of gas. h =pressure head. T=torque. S =speed of turbine. P_S= Shaft power.

AUTHOR'S PROFILE

Ali Hasan
born in Baghdad, Iraq 3/4/1963. M.Sc. degree Engineering, Hallam University, UK, 1993.Current employer; Senior Engineer, KEO Consulting Engineers, POB 18108, Doha, Qatar.

Abdelkader Benzamia,
Poiteriers France, 04/06/1978. M.Sc. degree Fluid Mechanics, University of Poitiers, France, 2004.Current employer; Head of Department, Flowpak, POB 8697, Doha, Qatar.